GeoVirtual 2020 September 14-16
Resilience and Innovation

Historical aerial photographs and digital photogrammetry techniques to investigate the development and evolution of the Chin Coulee landslide in Alberta

Evan Deane, Renato Macciotta & Michael Hendry
Department of Civil and Environmental Engineering – University of Alberta, Edmonton, AB, Canada
Chris Gräpel
Klohn Crippen Berger Ltd., Edmonton, AB, Canada
Roger Skirrow
Alberta Transportation, Edmonton, AB, Canada

ABSTRACT
The Chin Coulee landslide is situated on the northern slope of the Chin Coulee reservoir, Southern Alberta. The landslide has a volume of approximately 2 million cubic meters and Alberta Highway 36 is located upslope from the crest of the landslide. This highway has been affected by landslide retrogression to the extent that realignment has been necessary to maintain the highway operational. Alberta Transportation actively monitors the Chin Coulee landslide, however, resource allocation for geohazard management needs to meet public safety and highway operation requirements, as well as resource availability. Understanding the landside mechanisms, triggers and potential evolution are fundamental for defining cost/effective management strategies. This paper presents the use of historic aerial photographs in combination with modern digital photogrammetry tools to investigate the development of the Chin Coulee landslide, and its evolution towards its current state. This approach makes use of important legacy information available in the province.

RÉSUMÉ
Le glissement de terrain de Chin Coulee est situé sur le versant nord du réservoir de Chin Coulee, Alberta. A un volume d'environ 2 millions de mètres cubes et la route 36 de l'Alberta est située en amont de la crête du glissement de terrain. Cette route a été affectée par la régression des glissements de terrain dans la mesure où un réalignement a été nécessaire. Alberta Transportation surveille activement le glissement de terrain de Chin Coulee, cependant, l'allocation des ressources pour la gestion des géorisques doit répondre aux exigences de sécurité publique et d'exploitation des routes, ainsi qu'à la disponibilité des ressources. Comprendre les mécanismes côté terre, les déclencheurs et l'évolution potentielle sont fondamentaux pour définir des stratégies de gestion rentables / efficaces. Cet article présente l'utilisation de photographies aériennes historiques en combinaison avec des outils modernes de photogrammétrie numérique pour étudier le développement du glissement de terrain de Chin Coulee et son évolution vers son état actuel. Cette approche utilise des informations importantes sur l'héritage disponibles dans la province.

1 THE CHIN COULEE LANDSLIDE

The Chin Coulee landslide is described in Dean et al. (2019). The landslide is situated on the northern slope of the Chin Coulee reservoir, adjacent to Alberta Highway 36 (Figure 1). The Chin Coulee valley is approximately 55 m deep and 550 m wide at reservoir level. Natural valley slope inclinations vary but are generally about 6H:1V (9°). Highway 36 is a rural two-lane paved highway with average annual daily traffic of 880 vehicles (Government of Alberta, 2017). Headscarp retrogression threatens Highway 36, and loss of the roadway at this location would result in a detour length of about 25 km to the nearest crossing of Chin Coulee. An Aerial view of the landslide is shown in (Figure 2).

The slide is about 350 m wide and up to 45 m deep. The length of the slide is approximately 200 m long with the toe of slide within the reservoir. The total slide volume is estimated at approximately 2 million cubic meters, based on measurement along the proposed failure plane and current landslide extents.

A significant local realignment of the highway was performed in 2016, and a major regional realignment would be required if highway damage continues. A major

realignment would shift the road more than 50 m, outside the landslide zone entirely. This realignment is also contingent on reconstruction of the causeway, anticipated in 2030. Monitoring of landslide progression is ongoing, and evaluating landslide mitigation options until realignment occurs requires understanding the landside mechanisms, triggers and potential evolution.

1.1 Geology and Landslide Characteristics

The Chin Coulee valley is a glacial meltwater channel incised though a thick layer of stagnant ice moraine (till materials) and into Foremost Formation bedrock (Fenton et al., 2013 & Prior et al., 2013). The Foremost Formation is a unit within the Belly River Group stratigraphic unit of the late Cretaceous Western Canadian Sedimentary Basin. This bedrock unit consists of discontinuous layers of mudstones, clayey siltstones, silty shales, and sandstones (Dean et al. 2019).

Figure 1. Location of Chin Coulee Landslide in Alberta (base imagery from ESRI, 2019) (after Dean et al. 2019 with permission)

The local stratigraphy of the landslide is shown in Figure 3 for the cross section located in Figure 2. Medium plasticity clay fill material from the initial highway construction and subsequent realignments and regrading is exposed at the headscarp. A silty clay till with traces of fine gravel mantles the valley slope. The till has low to medium plasticity and is very stiff to hard. Thickness of the till varies from roughly 20 m at the toe of the slope to 35 m near the headscarp. Highly fractured shales and coal were encountered underneath the till.

1.2 Instrumentation at the Site and Landslide Kinematics

Standpipe piezometer and slope inclinometers were installed by Golder and Associates in 1998 (GA98-1 – 5) (Golder and Associates, 1998). Slope inclinometers and piezometers were installed by AMEC in 2002 and subsequently destroyed during a road and ditch realignment in 2012 (AMEC, 2013). Another slope inclinometer was installed by AMEC Foster Wheeler in 2015 (AMEC FW, 2015). Klohn Crippen Berger (KCB) installed two slope inclinometers between the highway and the head scarp in early 2018 to monitor for slide retrogression (KCB, 2018) (Dean et al. 2019).

Slope inclinometer concentrated zones of movement are shown in Figure 3. These, together with a low-strength coal seam were used to interpret the landslide kinematics. The Chin Coulee landslide has been interpreted as a translational retrogressive landslide seated within the highly fractured bedrock zone, sliding over a low-strength coal seam. Retrogression is inferred from surface tension cracks and concentrated deformations measured in slope inclinometer GA98-2 (Figure 3). Displacement rates vary between 10 and 50 mm/year.

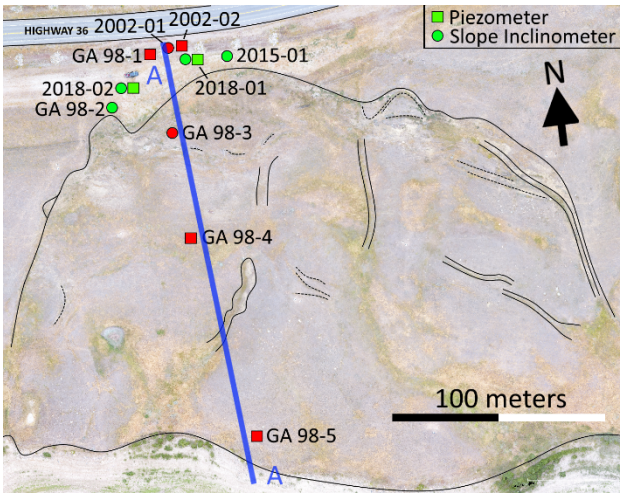

Figure 2. aerial view and instrument locations on Chin Coulee (Green symbols indicate currently functional instruments) (after Dean et al. 2019 with permission)

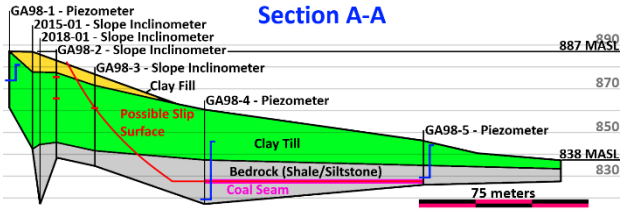

Figure 3. Chin Coulee Stratigraphy (Typical cross section). Red horizontal lines in slope inclinometer locations mark the depth of measured concentrated deformations (after Dean et al. 2019 with permission)

2 HISTORICAL AIR PHOTOS AND VISUAL INTERPRETATION

Historical air photos of the Chin Coulee landslide area are available from 1945 to 2012, roughly every 10 years. Table 1 shows the years and resolution of the air photos. These were obtained through the Alberta Air photo Library (https://www.alberta.ca/air-photos.aspx).

Table 1 Historical air photo year and resolution

Year	Resolution	No. overlapping photos
1945	1 in 20,000	4
1960	1 in 20,000	3
1970	1 in 30,000	3
1982	1 in 2,500	5
1993	1 in 30,000	2
1999	1 in 30,000	3
2012	1 in 30,000	2

Although the resolution of these photos varies significantly (between 1 in 30,000 and 1 in 2,500), they allow for inspection of the general features of the landslide area for a qualitative interpretation of landslide evolution. Figures 4 through 9 present a view of these photographs and main features in the area.

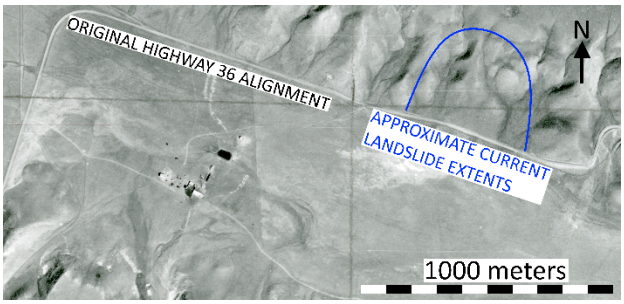

Figure 4. 1945 Air photo of Chin Coulee (Alberta Air photo Library, 1945) (after Dean et al. 2019 with permission)

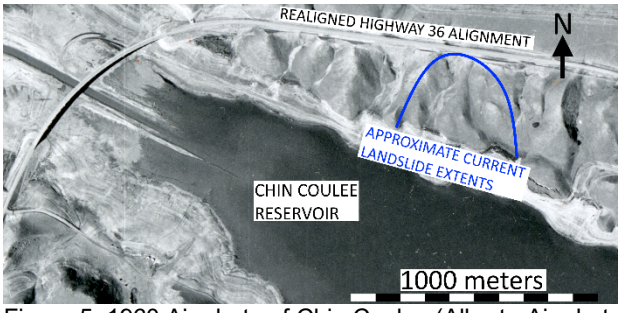

Figure 5. 1960 Air photo of Chin Coulee (Alberta Air photo Library, 1960) (after Dean et al. 2019 with permission)

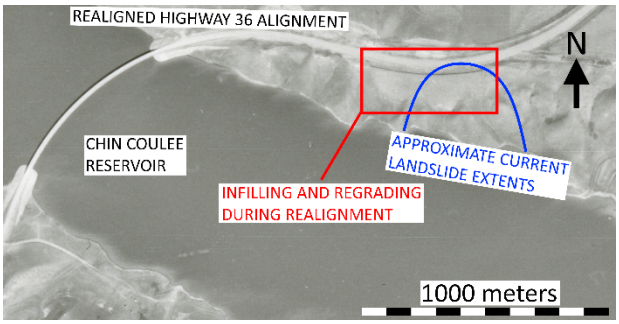

Figure 6. 1970 Air photo of Chin Coulee (Alberta Air photo Library, 1970) (after Dean et al. 2019 with permission)

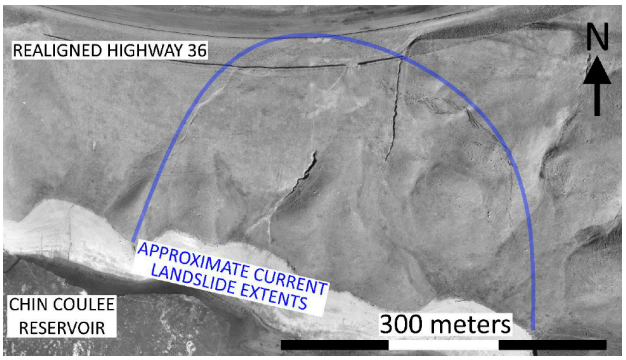

Figure 7. 1982 Air photo of Chin Coulee (Alberta Air photo Library, 1982)

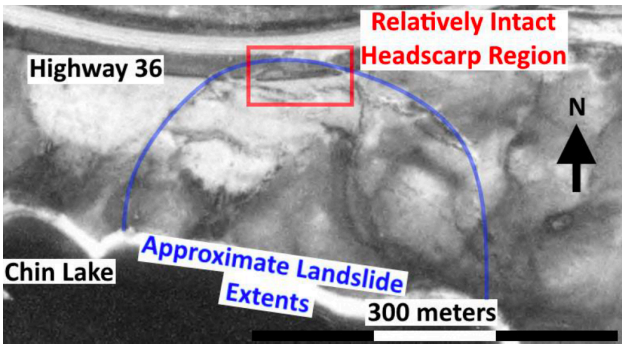

Figure 8. 1993 Air photo of Chin Coulee (Alberta Air photo Library, 1993)

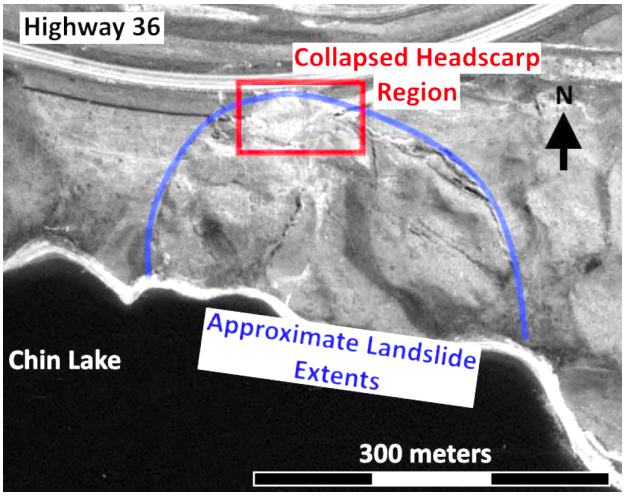

Figure 9. 1999 Air photo of Chin Coulee (Alberta Air photo Library, 1999)

2.1 Interpretation of landslide development and evolution

The historical air photos create a visual timeline of landslide evolution and allow for historical monitoring of landslide movement and identification of major movement events and their correlation with external events, such as highway construction and reservoir impoundment.

Prior to 1960, the only anthropogenic impact on the natural slope environment of the present-day Chin Coulee

landslide was the cut required to accommodate the original alignment of Highway 36 (toe of the slope – Figure 4).

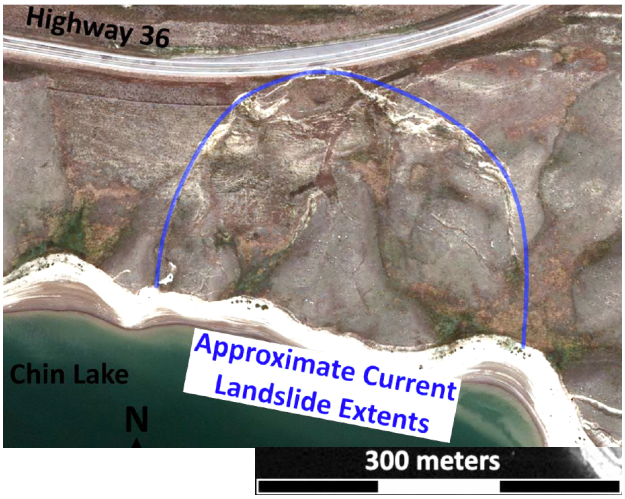

Figure 10. 2012 Air photo of Chin Coulee (Alberta Air photo Library, 2012)

Air photos taken in 1960 show the realigned Highway 36, which was raised out of the valley floor, up the slope, and above the current landslide extents in the mid 1950's as the reservoir began to fill. Based on inspection of the 1960 air photos, this highway realignment did not require significant cuts or infilling (See Figure 5). No slope disturbance was visible within the landslide extents at this time. Some anthropogenic influence on the landslide due to reservoir fluctuations could have initiated at this stage.

Between 1960 and 1970, Highway 36 was realigned to create an arc to connect onto a pre-existing northbound range road. During this realignment the highway section directly above the landslide was relocated south and a berm was created within the current landslide extents with infilled materials and regraded (Figure 6). This major change in topography was identified by AMEC as a potential cause for slope instability due to restriction of drainage (AMEC 2000). It is understood that this configuration increased the loading on the slope and provided for a steeper configuration. Reservoir management would have also created episodes of ground water increases within the landslide body, potentially followed by rapid drawdown conditions. No slope instability was visible within the landslide extents at this time. Based on air photo interpretation, water levels within the Chin reservoir appear to be similar to modern day levels at this time, which suggests an increase in pore pressures compared to the original configuration (no reservoir).

In the fall of 1978 a significant slope failure of the Chin Coulee landslide and associated undermining of the northbound shoulder was identified by Alberta Transportation (Golder and Associates 1998). Figure 7 shows the first air photo after the initial failure, taken in 1982. Scarp formations are visible around the periphery of the current landslide region. Movement is most significant in the upper right, with less movement along the left side of the landslide. Lateral cracks are visible and start to delineate what is the current landslide extent.

Landslide movement continued between 1982 and 1993 with scarp regions on the left and right of the active zone showing significant deformations (Figure 8). The quality of this photo is lower compared to other photo sets, however some observations can be made. The headscarp region does not appear disturbed, however a close inspection reveals tension crack formation at the edge of the road, potentially the start of undermining of the guardrails and road structure.

In 1997 Alberta Transportation reported significant undermining of the northbound lane on Highway 36 and began continuous annual monitoring of the Chin Coulee landslide in 1998. Figure 9 shows a large block near the headscarp which collapsed between 1993 and 1999.

Figure 10 shows well defined landslide boundaries as of 2012. This figure shows that Highway 36 was slightly realigned northwards at the location of the landslide scarp as a response to undermining of the northbound lane.

3 PHOTOGRAMMETRY WITH HISTORICAL AIR PHOTOS

Aerial photography has a long history of use in engineering. Linear infrastructure design has taken advantage of large data sets of historical air photos to plan road, pipeline, and powerline construction projects. Stereo pairs are used extensively in geomorphology studies and preliminary characterization of surface materials. The availability of modern software tools for photogrammetry (e.g. Pix4DMapper, Autodesk ReCap, AdamTech, Agisoft Metashape, Regard3D) has allowed for aircraft, UAV and ground-based photogrammetry to become a standard tool for geohazard management. These tools allow working with digitized air photos (high-quality scans), which opens the door to building 3-dimensional surface models from historical air photos (Macciotta et al. 2017). In turn, these could be compared to varying configurations the landslide throughout its history.

3.1 Digital surface model from historical air photos

Digital photogrammetric techniques were applied for the historic photographs of the Chin Coulee landslide. The software used was Pix4D (https://www.pix4d.com/). Challenges encountered included:

- Photograph scales of 1 in 20,000 and 30,000 proved inadequate for the dimensions of the landslide, not allowing the detailed topography to be modelled,
- Digital construction of topographic surfaces based on air photos improves with increasing number of overlapping photographs. Most years had 2 or 3 overlapping photos at the site with only 1982 providing 5 overlapping photos,
- Incompatibility exists between the resolution of topography derived from photographs at different scales and with topography derived from modern techniques such as UAV photogrammetry, LiDAR (laser scanning).

Attempts on historical photos at this site for scales of 1 in 20,000 and smaller were not successful, and work is ongoing to implement algorithms that can provide useful topographic features from these photos. A detailed, 3-dimensional topographic model was successfully obtained from the 1982 set of photographs (Figure 11).

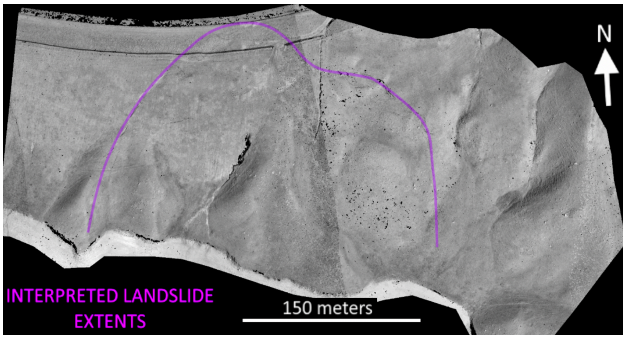

Figure 11 View of the 3-dimensional topographic model constructed from 1982 historical photographs

Historical air photo photogrammetry is limited due to the absence of ground control points (GCPs). GCPs are points of known coordinates (global or relative coordinates) that allow scaling the surface models and improving the accuracy of the models. Modern photography for photogrammetry takes advantage of GPS systems mounted in the cameras and surveying of control points in the ground. Identification of structures which could act as GCPs in historical photos is possible, however this often requires the assumption that these structures or objects have not moved in the time span between when the photo was taken and when the object was geolocated.

Several large rocks were identified in the 1982 photos and in UAV photos and LiDAR scans in 2018 and 2019. These were used as GCPs in the creation of the 1982 photogrammetry model shown in Figure 11. This was possible due to the high resolution of the 1982 photos and was not possible with lower resolution air photos. An important limitation is the assumption that these blocks would not have moved since 1982. This was considered adequate relative to the amount of deformation of the landslide.

3.2 Historical air photo surfaces for quantifying slope changes

The availability of the topographic surface derived from the 1982 air photographs provided the opportunity for a quantitative comparison of surface changes between 1982 and 2019. Comparison was done through change detection techniques. Change detection is based on the process of using temporally separated detailed topographies to detect variation over time (Jaboyedoff et al. 2012). Typically, these surfaces are represented by point clouds obtained through laser scanning (LiDAR) or photogrammetry. These point clouds are aligned by matching areas considered stable, and the separation between point clouds within areas of expected movement is calculated. The software used for converting the 1982 photogrammetric model to point cloud was Pix4D, sampling the model such that there are at least 500 points per m^2. The software used for point cloud analysis and change detection was CloudCompare V2.10 (www.cloudcompare.org). The method used for change detection was M3C2 (Lague et al. 2013). Change is quantified as the distance between point clouds measured parallel to the normal vector of the surface in the vicinity of each measurement point.

A LiDAR Scan from July 29th, 2019 was selected for comparison. Selection corresponded to the latest scan obtained for this research. Scanning was performed with an Optech ILRIS-LR laser scanner (Teledyne Optech 2019) with an approximate ground point spacing of 20 – 30 mm.

Alignment of the two point clouds aimed to achieve the closest match between areas considered stable. After the alignment process, the relative change between the clouds, within the stable areas, can be calculated and a distribution of change is obtained. This distribution should be centred in zero. In this research, two standard deviations was adopted as the threshold for change detectability, or limit of detection (LOD). This means that any change calculated within +/- two standard deviations was considered potential measurement randomness. The limit of detection between the 1982 photogrammetric model and the 2019 LiDAR model was 1 m. This significant limit can be attributed to a lower accuracy of the 1982 model derived from historic photos and surficial changes between 1982 and 2019 due to erosional processes (precipitation, freeze-thaw, etc.) and surficial soil movements. The calculated change between the 1982 historical photograph 3-dimensional model and the 2019 LiDAR point clouds is presented in Figure 12.

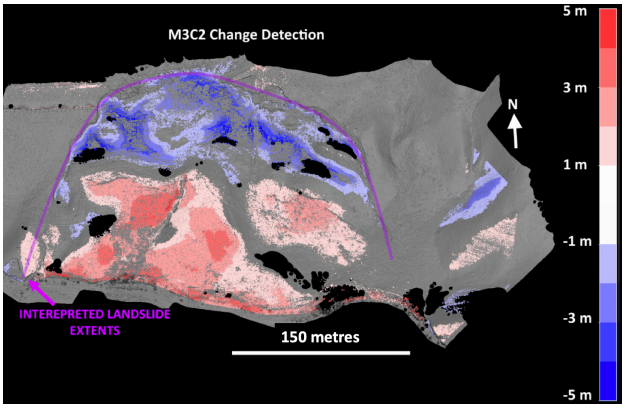

Figure 12 Calculated change between the 1982 historical photograph 3-dimensional model and the 2019 LiDAR point clouds

Figure 12 indicates considerable loss of material in the upper half of the slope of approximately 4 m between 1982 and 2019. The order of magnitude of this change is confirmed by inspection of the landslide scarp when compared to a 2.5 m high fence (Figure 13). Although differences in resolution and accuracy between the models, this comparison increased the confidence in the

magnitudes of the calculated change for interpretation purposes.

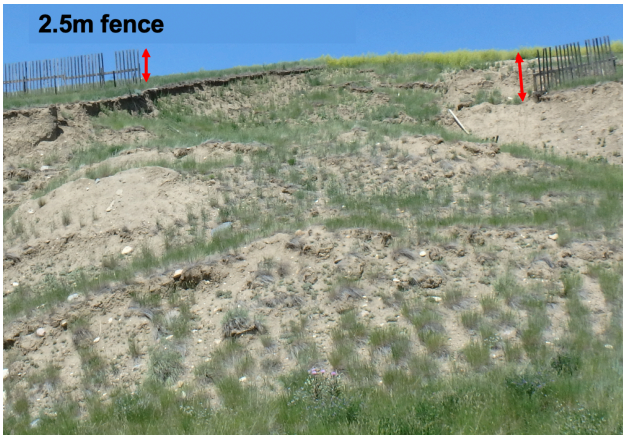

Figure 13 View of the upper half of the Chin Coulee landslide showing a 2.5m high fence as reference scale for the dimensions of the back scarp

Changes in the lower half of the landslide show outward movement of the slope between 2 and 3m, with some areas showing up to 4m differences. More importantly, the transition between the areas showing material loss and the toe showing outward displacement is sudden.

Rotational failures tend to show height drops in the upper section of the landslide (which would be translated as material loss in change detection) transitioning towards rotation (associated with very little change identified by change detection) and further to outward movements near the toe of the landslide. Translational slides tend to show homogeneous change, or very little change if the sliding surface is parallel to the topography of the slope. In the case of the Chin Coulee landslide deformation is consistent with that of compound slides where an active wedge moves downward pushing a passive wedge outward on a sub-horizontal shear zone. Material loss in the upper half indicates downward movement of a potentially driving wedge, the sharp change to outward movement indicated the location of the contact between the driving and passive wedges, and the area showing outward change corresponds to the passive wedge.

4 CONCLUSIONS

Aerial photography has a long history of use in engineering, particularly in geomorphology and for geohazard assessments. With photogrammetric techniques now part of the state of practice in geotechnical engineering, a door opens towards extracting enhanced historic information from legacy aerial photography. This paper presents the use of historic aerial photographs in combination with modern digital photogrammetry tools to investigate the development of the Chin Coulee landslide, and its evolution towards its current state. This approach makes use of important legacy information available in the province.

Development of digital 3-dimensional topographic models enhance the capability of the practitioner to observe landslide features and temporal changes from diverse perspectives. Further, it can allow for the development of stability models, granted the uncertainties in model accuracy, for past configurations when no other information is available.

In this paper, the distance between 1982 aerial photography and 2019 ground-based laser scanning was calculated. Both point clouds were originated from different techniques and had incompatible resolution, however it was decided to adopt the criteria of sampling both models to a minimum of 500 points per m^2 to allow for statistical calculations of distance between the point clouds through the M3C2 method. The resulting change was compared against visual inspection of the features on site, which increased the confidence in the magnitude of the calculated changes. More importantly, the results allowed to better define the kinematics of the landslide as a compound slide with a driving wedge moving downwards and pushing a passive wedge outward into the reservoir. Also, the results identified the location of the contact between the driving and passive wedges.

The work in this paper highlights that novel techniques for landslide investigation, particularly building 3-dimensional surface models and change detection, can be applied to historical aerial photography to increase the information available for understanding the evolution of landslides.

5 ACKNOWLEDGMENTS

The authors would like to acknowledge Hanh Hong (formerly Klohn Crippen Berger), Jorge Rodriguez (University of Alberta), as well as the graduate students and research associates at the university of Alberta that supported some of the field work associated with this research.

6 REFERENCES

Alberta Air photo Library. 1945 Flight Index A7764(6).
Alberta Air photo Library. 1960. Flight Index YC414(52).
Alberta Air photo Library. 1970. Flight Index AS1052(24).
Alberta Air photo Library. 1982. Flight Index 2448(144).
Alberta Air photo Library. 1993. Flight Index AS4404(85).
Alberta Air photo Library. 1999. Flight Index AS4955(258).
Alberta Air photo Library. 2012. Flight Index 2012021(705).
AMEC. 2013. Instrumentation Monitoring Results – December 2013 Report, *Geotechnical Risk Management Plan*.
AMEC FW. 2015. Instrumentation Monitoring Results – December 2015 Report, *Geotechnical Risk Management Plan*.

Deane, E., Macciotta, R., Hendry, M., Gräpel, C., Skirrow, R. 2019. The use and limitations of modern technologies for slow vegetated landslide monitoring – Chin Coulee Landslide. In: Geo St. John's 2019, Proceedings of the 72nd Canadian Geotechnical Conference, September 29th – October 2nd, 2019, St. John's, NL.

Esri. 2019. Topographic and World Basemap. www.arcgis.com/home/item.html?id=30e5fe3149c34df1ba922e6f5bbf808f [April 19, 2019].

Fenton, M.M., Waters, E.J., Pawley, S.M., Atkinson, N., Utting, D.J., and Mckay, K. 2013. Surficial geology of Alberta; Alberta Energy Regulator, AER/AGS Map 601

Golder and Associates. 1998. Geotechnical Investigation – November 1998 Report, *Geotechnical Risk Management Plan*.

Government of Alberta. 2017. Alberta Highway 1 to 986 Traffic Volume History (2008 – 2017). www.open.alberta.ca/opendata/traffic-volumes-at-points-on-the-highway [April 25, 2019].

Jaboyedoff, M., Oppikofer, t., Abellán, A., Derron, M.H., Loye, A., Metzger, R. and Pedrazzini, A. 2012. Use of LIDAR in landslide investigations: A review. Natural Hazards 61(1): 5-28

KCB. 2018. Geotechnical Drilling and Instrument Installation – February 2018 Report, *Geotechnical Risk Management Plan*.

Lague, D., Nicolas, B., and Jérôme, L. 2013. Accurate 3D Comparison of Complex Topography with Terrestrial Laser Scanner: Application to the Rangitikei Canyon (N-Z). *ISPRS Journal of Photogrammetry and Remote Sensing,* 82: 10-26.

Macciotta, R., Rodriguez, J., Hendry, M., Martin, C.D., Edwards, T. and Evans, T. 2017. The 10-mile Slide North of Lillooet, British Columbia – History, Characteristics and Monitoring. In J. V. De Graff & A. Shakoor, eds. 3rd North American Symposium on Landslides. Roanoke, Virginia, pp. 937–948

Prior, G.J., Hathway, B., Glombick, P.M., Pana, D.I., Banks, C.J., Hay, D.C., Schneider, C.L., Grobe, M., Elgr, R., and Weiss, J.A. 2013. Bedrock geology of Alberta; Alberta Energy Regulator, AER/AGS Map 600

Teledyne Optech. 2019. ILRIS-LR Specifications Sheet. info.teledyneoptech.com/acton/attachment/19958/f-02ea/1/-/-/-/-/ILRIS-LR-Spec-Sheet_LR.pdf [April 22, 2019]